Eur Phys J A (2004) **19**, s01, 105–110
Digital Object Identifier (DOI) 10.1140/epjad/s2004-03-018-8

EPJ A direct
electronic only

Propagation of fast partons in the nuclear medium

Mikkel B. Johnson

Los Alamos National Laboratory, Los Alamos, NM 87544

Received: 30 Aug 2003 / Accepted: 14 Nov 2003 /
Published Online: 6 Feb 2004 – © Società Italiana di Fisica / Springer-Verlag 2004

Abstract. The color dipole approach has been applied in the target rest frame to address the issues of transverse momentum broadening and energy loss of a fast quark propagating in the nuclear medium. A recent application of the theory to the FermiLab E772/E866 experimental data, determining the rate of energy loss of a quark propagating in the medium to be 2 to 3 GeV/fm, will be reviewed. Calculations for the transverse momentum distribution will be presented, and the results will be compared to the E866 data. The theory will be shown to compare favorably to the data, and these results will be shown to suggest that the momentum broadening of a quark is about twice the generally accepted size.

PACS. 13.85.Qk; 24.85+p Drell-Yan processes; medium effects; heavy-ion collisions

1 Introduction

Nucleon-nucleus (or deuteron-nucleus) reactions at high energy are important experimentally because they constitute the conventional background for the less well known dynamics of relativistic nucleus-nucleus collisions, which have been identified as a means for producing the quark-gluon plasma in the labratory at facilities such as the Relativestic Heavy Ion Collider (RHIC) at BNL, and the Large Hadron Collider (LHC) at CERN. To develop sufficient confidence in theory to interpret the more complicated phenomena in nucleus-nucleus collisions, it is vital that the theory be tested against these simpler data first.

Shadowing, quark energy loss, and transverse momentum broadening are three central issues of parton propagation in nucleus-nucleus collisions that may be quantitatively addressed in p+A reactions, specifically in Drell-Yan (DY) reactions. The color dipole approach in the target rest frame provides an attractive means for interpreting these data to learn more about these phenomena. After a brief description of the status of this theory, I will review recent results that are improving our understanding of the physics behind these aspects of parton propagation in the nuclear medium.

Drell-Yan in the target rest frame may be described as a quark of the incident hadron interacting with a target nucleon, radiating a virtual photon $\gamma*$ of mass M that subsequently decays into the observed Drell-Yan dilepton pair $\bar{l}l$. In the target rest frame, the $\gamma*$ is a constituent of projectile fluctions, which are "frozen" by time dilation for a length of time t_c given by the uncertainty relation,

$$t_c = \frac{2E_q}{M^2_{q\bar{l}l} - m_q^2} \tag{1}$$

where E_q and m_q refer to the energy and mass of the projectile quark and $M^2_{q\bar{l}l}$ is the square of the effective mass of the fluctuation,

$$M^2_{q\bar{l}l} = \frac{m_q^2}{\alpha} + \frac{M^2}{1-\alpha} + \frac{k_T^2}{\alpha(1-\alpha)}, \tag{2}$$

where α is the fraction of the light-cone momentum of the incident quark carried by the lepton pair, and k_T^2 is the square of the transverse momentum of the lepton pair. The fluctuation lifetime t_c is called the coherence time, and the DY reaction occurs when the $\gamma*$ of the fluctuation is released by an interaction between one of the constituents of the fluctuation and a target nucleon. In the color dipole approach, this interaction is mediated by the color dipole cross section, $\sigma_{\bar{q}q}$.

When the scattering takes place on a nucleus, multiple interactions with target nucleons can give rise to various medium effects. Two limiting cases should be distinguished, the short coherence length limit (SCL) reached when the coherence length $\ell_c \equiv c\langle t_c\rangle$ is much smaller than the interparticle spacing d, $\ell_c \ll d$ (in a heavy nucleus, $d \approx 2fm$), and the long coherence length limit (LCL) reached when $\ell_c \gg R_A$, where R_A is the nuclear radius. The coherence length determines the physics and also controls the way that medium effects are taken into account. The theory simplifies these important limits. The intermediate case is generally more difficult to describe; however, if $0 < \ell_c \ll R_A$, the result can be obtained by interpolating between these limits using the square of the longitudinal form factor, $F_A^2(q_c)$, where $q_c = 1/l_c$ is the longitudinal momentum transferred in the reaction. The Green function method [1] was developed to handle the more difficult situations. Our results make use of all these cases.

One important medium effect is shadowing, and a basic consideration is the connection between shadowing and the coherence length. In the SCL there is no shadowing because the duration of the fluctuation is so short that it has no time to interact with the medium. In the LCL, which is applicable to reactions at the LHC and at RHIC under certain kinematic conditions, there is maximal shadowing.

Medium effects also give rise to quark energy loss and to transverse momentum broadening. These both arise in the SCL as the quark from the incident hadron undergoes various additional interactions with nucleons of the nucleus before it radiates the $\gamma*$. For the LCL, the quark may undergo interactions that lead not only to shadowing but also to additional momentum broadening. Nuclear effects giving rise to momentum broadening and shadowing are believed to arise predominantly from the same color dipole cross section $\sigma_{\bar{q}q}(r_T)$ that mediates the DY reaction on a nucleon.

The DY data relevant to shadowing, energy loss, and momentum broadening in which we are interested here is the $p + A$ FermiLab data from the E772/E866 collaboration. This data corresponds to the range of coherent length where the shadowing is weak and the interpolation formula described above applies.

2 Drell-Yan reaction on a nucleon in the target rest frame

In the color dipole approach, the Drell-Yan reaction occurs when a fast projectile quark scatters off the gluonic field of the target, as shown in Fig. 1. The color dipole approach was originally proposed for deep-inelastic scattering (DIS). Extension to Drell-Yan was developed by Kopeliovich [2] and subsequently by Brodsky, et al. [3]. The DY reaction on a nucleon is described by

$$M^2 \frac{d^2\sigma_{DY}}{dM^2 dx_1} = \int_{x_1}^1 dx_q F_q^h(x_q) \int d^2\rho |\Psi(\alpha,\rho)|^2 \sigma_{\bar{q}q}(\alpha\rho), \tag{3}$$

where $\sigma_{\bar{q}q}$ is the color-dipole cross section, ρ is the transverse distance between the $\gamma*$ and quark in the fluctuation, and Ψ represents the distribution for the incident quark to fluctuate into a quark and the $\gamma*$. In DY, the color dipole consists of the quark before and after the release of the $\gamma*$, whose impact parameters differ by $\alpha\rho$. Here $x_q(x_1)$ is the fraction of light-cone momentum of the incoming hadron h (for us a proton) carried by the quark (lepton pair); the light-cone momentum fraction α is given in terms of these variables, $\alpha = x_1/x_q$; and, F_q^h is the quark distribution function of the incident hadron.

Deep-inelastic scattering from nucleons at HERA at DESY has been used to fix models of the color-dipole cross section. The HERA data suggests saturation, the condition that the color dipole cross section approaches a constant value at large r_T,

$$\sigma_{\bar{q}q}(r_T) = \sigma_0(1 - e^{-r_T^2/R_0^2}). \tag{4}$$

Models that incorporate this saturation property include the GW [4] and KST [5] models. We see that in both the GW and KST models, for small r_T,

$$\sigma_{\bar{q}q}(r_T) \approx C r_T^2, \tag{5}$$

where $C = \sigma_0/R_0^2$ is a constant that depends on the quark energy, in the case of the KST model, and on Bjorken x in the case of the GW model. For us, the most important point is that once the color dipole cross section has been fit to experimental DIS data on the nucleon, the color-dipole formalism makes predictions for Drell-Yan both in nucleon-nucleon [6] and nucleon-nucleus scattering with no further adjustment of parameters.

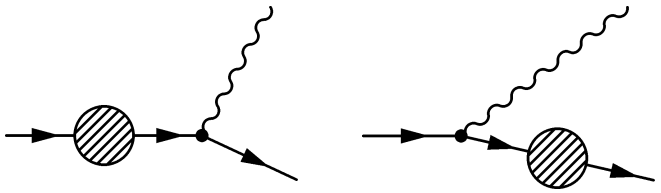

Fig. 1. In the target rest frame, DY dilepton production looks like bremsstrahlung. A quark or an anti-quark from the projectile hadron scatters off the target color field (denoted by the *shaded circles*) and radiates a massive photon, which subsequently decays into the lepton pair. The photon decay is not shown. The photon can be radiated before or after the quark scatters

The theory is expected to be valid for small Bjorken x only, and specific calculations [6] have shown it to agree well for $x_2 < 0.1$ in both the magnitude and shape with the next-to-leading order parton model. Although the calculations disagreed with the E772 FermiLab data, they are in excellent agreement with the more recent E866 analysis in [7].

3 Medium effects in DY reactions for p+A collisions in the target rest frame

Medium effects are evident in nuclear ratios of cross sections $R^{A/A'}$. These include analyses of both cross sections themselves, and the analysis of momentum distributions. For each, there are two cases of interest: weak shadowing and maximal shadowing.

As we have stated, shadowing is controled by the coherence length, and explicit calculations in [8] show that for incident quarks of the 800 GeV projectile protons the coherence length is quite a bit less than the nuclear radius, implying weak shadowing. Additionally, these calculations show that the coherence length of the dominant $q-\gamma*$ fluctuation is nearly constant as a function of x_1 and is therefore essentially a function of x_2 alone. For $x_2 > .03$, $\ell_c < 2$ fm, and shadowing can be safely ignored. For smaller x_2 the coherence length exceeds the interparticle spacing at the center of the nucleus, and shadowing therefore begins to become important. The particular admixture of long- and short-coherence length contributions is determined by the longitudinal form factor, as stated in the introduction, and this depends in turn explicitly on the variation of ℓ_c with x_1 and x_2.

For cross section ratios,

$$R^{A/A'} = \frac{d^2\sigma^A_{DY}}{dM^2dx_1}/\frac{d^2\sigma^{A'}_{DY}}{dM^2dx_1}, \tag{6}$$

the E772/E866 FermiLab data at $E_p = 800\ GeV$ has been used for a recent determination of quark energy loss [8]. The DY reaction at RHIC for $x_F = x_1 - x_2 > 0.5$ and at the LHC lies in the regime of long-coherence length physics, and such experiments at these facilities will be exploring a limit that has so far not been accessible experimentally. Predictions of cross sections in $p+A$, $d+A$, and $A+A$ collisions [9] have been made recently in the latter case.

For momentum distribution ratios,

$$R^{A/A'}(p_T) = \frac{d^2\sigma^A_{DY}}{dp_T^2}/\frac{d^2\sigma^{A'}_{DY}}{dp_T^2}, \tag{7}$$

data relevant to the the case of weak shadowing has been taken at $E_p = 800\ GeV$ by the FermiLab E772/E866 collaboration and was used by them to study quark momentum broadening in nuclei,

$$\delta\langle p_T^2\rangle = \langle p_T^2\rangle^A - \langle p_T^2\rangle^p. \tag{8}$$

This same regime is relevant to $p+A$ collisions at RHIC. The case of maximal shadowing is relevant to the LHC and RHIC, and predictions are made in [9].

3.1 Cross section ratios

Let us consider first the case of weak shadowing for the cross section ratios, as analyzed in [8]. To calculate the cross section, we must calculate the cross section separately in the SCL and LCL and then interpolate between them using using the longitudinal form factor, as explained in the introduction.

The main medium effect in the short coherence length limit $x_2 \gg 0.03$ the $\gamma*$ is the quark energy loss, which occurs before the $\gamma*$ is radiated. The interactions that cause the incident quark to lose energy reduce the quark momentum fraction x_q and hence shift the value of $x_1 = \alpha x_q$. The amount of reduction due to quark energy loss may be calculated as $x_q \approx E_q/E_h \to x_q - \kappa L/E_h$, where L is the path length of the incident quark in the nucleus and κ is its rate of energy loss. Using these kinematic considerations, we find an expression in [8] for the DY cross section $M^2\frac{d^2\sigma^{(SLC)}_{DY}}{dM^2dx_1}$ including its dependance on κ. It becomes sensitive to κ for $x_1 \approx 1$.

Mechanisms of energy loss [8] consist of the primary ones of string breaking (SB), for which $\kappa_{SB} \approx 1\ GeV/fm$ (numerically, the string tension), and the independent process of gluon radiation (GR), for which $\kappa_{GR} \approx 3\alpha_s\langle k_T^2\rangle \approx 0.8\ GeV/fm$, where $\langle k_T^2\rangle \approx 0.65\ GeV$ is the mean-square momentum of the radiated gluon. The induced energy-loss mechanisms arising from multiple interactions with nucleons are relatively minor for nuclei of ordinary density and can be neglected. We thus expect that $\kappa \approx 1.8\ GeV/fm$.

As we have said, shadowing arises in the LCL through multiple interactions between the quark and the nucleus following the emission of the $\gamma*$. For weak shadowing, Glauber theory to second order in the number of interactions may be used, giving

$$M^2\frac{d^2\sigma^{(LCL)}_{DY}}{dM^2dx_1} = \langle\sigma_{\bar{q}q}(\alpha\rho)\rangle(1 - \frac{\sigma_{eff}\langle T_A\rangle}{4}) \tag{9}$$

where the brackets around the color dipole cross section refer to the averages over (ρ,α) in (3), and where $\langle T_A\rangle$ is the average of the thickness function $T_A(b)$ over impact parameter b,

$$< T_A >= \frac{1}{A}\int d^2bT_A^2(b), \tag{10}$$

with $T_A(b) = T_A(b,\infty)$, where

$$T_A(b,z) = \int_{-\infty}^{z} d^2b\rho_A(b,z), \tag{11}$$

and $\rho_A(b,z)$ is the nuclear density. The quantity $\sigma_{eff} = \langle\sigma^2_{\bar{q}q}\rangle/\langle\sigma_{\bar{q}q}\rangle$ in (9) is obtained by expanding the multiple scattering through second order in $\sigma_{\bar{q}q}$. In the color-dipole approach shadowing is completely determined by the color dipole cross section when shadowing is weak.

Interpolating between the LCL where $x_2 \ll 0.03$ and the SCL where $x_2 \gg 0.03$, we obtain

$$\frac{d^2\sigma_{DY}}{dM^2dx_1} = \frac{d^2\sigma^{(SCL)}_{DY}}{dM^2dx_1}(1 - F_A^2(q_c)) + \frac{d^2\sigma^{(LCL)}_{DY}}{dM^2dx_1}F_A^2(q_c), \tag{12}$$

where $q_c = 1/\ell_c$ and the longitudinal form factor is defined as

$$F_A^2(q) = \frac{1}{< T_A >}\int d^2b|\int_{-\infty}^{\infty} dze^{iqz}\rho(b,z)|^2. \tag{13}$$

Note that this interpolation formula has the correct limits for $\ell_c \to 0$ and $\ell_c \to \infty$. It also correctly reproduces the Gribov shadowing formula [10,11] and correctly describes shadowing in DIS [8]. Because the cross section becomes sensitive to both shadowing and κ for $x_1 \approx 1$, it is important that both effects are included in the theory (note that the depencence of shadowing on ℓ_c becomes quite intricate in this limit [12,8]). This theory then provides a quantitative test of the value of the relatively poorly known quark energy loss in the nuclear medium, since shadowing is completely determined by theory.

For comparing the theory to experiment, we have evaluated (12) and compared to the E866/E772 FermiLab data. This data provides the dependence of $R^{A/A'}$ over a range of (A, x_1, M^2); our ability to reproduce these data gives us confidence that we are able to separate the effects of shadowing and energy loss. Typical results are shown in Fig. 2.

The rate of energy loss corresponding to the fit to the the data, as shown in Fig. 2, is

$$\kappa = 2.73 \pm 0.37 GeV/fm \tag{14}$$

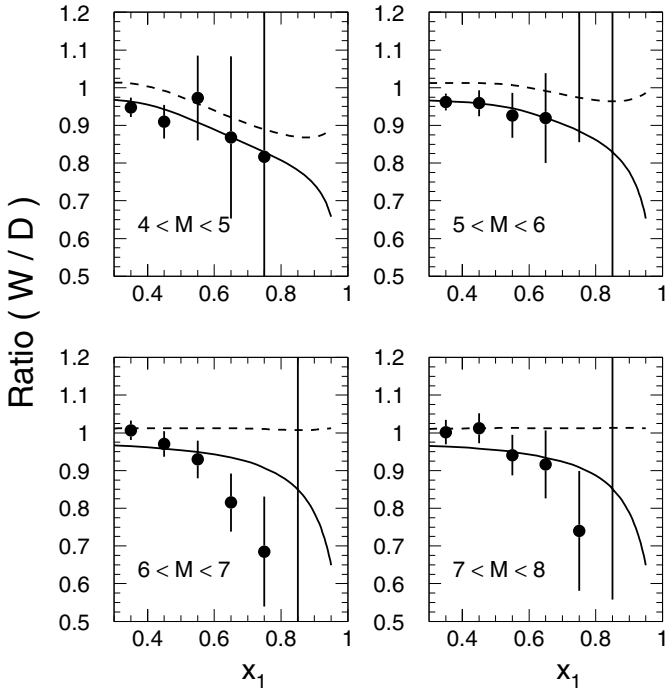

Fig. 2. Examples of ratios of the DY cross sections of tungsten to deuterium as functions of x_1 for various intervals of M. *Dashed curves* correspond to net shadowing contribution, *solid curves* show the full effect including shadowing and energy loss. Data are from [13,14]

Note that the value in (14) is somewhat larger than the theoretical estimate of 1.8 GeV/fm given above; it is also considerably larger than values found in previous analyses of the DY data [15]. We regard our value as more reliable, since the color dipole approach is able to disentangle shadowing from energy loss using a reliable theoretical calculation of the shadowing contribution.

3.2 Momentum distribution ratios [16]

Calculations show that the momentum distributions from E772/E866 experiments with $800GeV$ protons or measurements at RHIC with $s^{1/2} = 200\ GeV$ protons at $x_F = 0$ correspond to the short coherence length limit, as long as $x_2 > 0.05$. Working in the short coherence length limit simplifies the theory by eliminating the shadowing term in (12). We will restrict our attention to this kinematic regime, which is possible because the data is available binned in x_2 intervals, and thus concentrate on the first (LCL) term in this expression.

It was recognized in [17] that at high energies, the multiple interaction of a quark propagating in the nuclear medium can be eikonalized and exponentiates into a factor containing the color dipole cross section and nuclear thickness function. The physics of momentum broadening of the quark is therefore that of color filtering, or absorption of large dipoles leading to diminished transverse separation with distance. Then, the probability distribution $W^A(k_T)$ that a quark will have acquired transverse momentum k_T at a position (b, z) in the nucleus A becomes [17]

$$W^A(k_T) = \frac{1}{(2\pi)^2}\int d^2r_T e^{ik_T\cdot r_T} e^{-\frac{1}{2}\sigma_{\bar{q}q}(r_T)T_A(b,z)}, \quad (15)$$

where $T_A(b, z)$ is defined in (11). We express the cross section, $\sigma^A_{DY}(p_T)$, for a proton to produce a DY pair on a nucleus A with transverse momentum p_T as convolution of the probability $W^A(k_T)$ and the DY momentum distribution on a proton. The resulting expression entails an integral over $\Psi(\alpha, \rho)$ as in (3), and for the results we show below, this integral has been performed numerically. However, for the purpose of discussing the result here, we replace the quantities that depend on α by averages. Then, the ratio $R^{A/p}(p_T)$ may be expressed as in terms of the DY cross section $\sigma_{DY}(p_T)$,

$$R^{A/p}(p_T) = \frac{1}{\sigma^p_{DY}(p_T)}\int d^2k_T W^A(k_T)\sigma^p_{DY}(p_T - \bar{\alpha}k_T) \quad (16)$$

where $\bar{\alpha}$ arises from the fact that the DY pair carries away a fraction α of the transverse momentum of a quark in the incident proton. We find that $\bar{\alpha} = \langle\alpha^2\rangle^{1/2} \approx 0.97$. The average over α implicit in (16) also entails an evaluation of the quark energy, $\langle E_q\rangle \approx E_q/3$, since we use the GW model of $\sigma_{\bar{q}q}$, which depends explicitly on this energy.

For our calculations below we have chosen

$$\sigma^p_{DY}(p_T) \propto (1 + p_T^2/\Lambda^2)^{-6} \quad (17)$$

where the value of $\Lambda^2 = 7GeV^2$ is taken from [18].

Some of the integrals in (15, 16) may be done analytically by expanding out the exponential in (4). We find that to an excellent approximation, the effect of averaging (15) over (b, z) is to replace

$$T_A(b, z) \to \langle T_A\rangle/2. \quad (18)$$

When evaluating (15), we also take into account gluon shadowing by replacing $\sigma_{\bar{q}q} \to R_G\sigma_{\bar{q}q}$, where R_G is the gluon shadowing function. See [17] for more discussion. Our calculations are however insensitive to R_G.

Our calculation for $R^{W/Be}(p_T)$ is shown in Fig. 3. The data relevant to p_T distributions on nuclei are FermiLab E772/E866 data [15,14,19]. One sees that the calculation is in quite good agreement with experiment. Note that the details of the Cronin effect, the rise above 1 for $p_T \approx 3$ in Fig. 3, are completely explained with no adjustable parameters. We find comparable agreement with $R^{Fe/Be}(p_T)$.

3.3 Transverse momentum broadening

The transverse momentum broadening of a quark propagating in a nucleus is defined in (8) where the mean momentum is defined as

$$\langle p_T^2\rangle = \frac{\int d^2_{pT}p_T^2\sigma^A_{DY}(p_T)}{\int d^2_{pT}\sigma^A_{DY}(p_T)}. \quad (19)$$

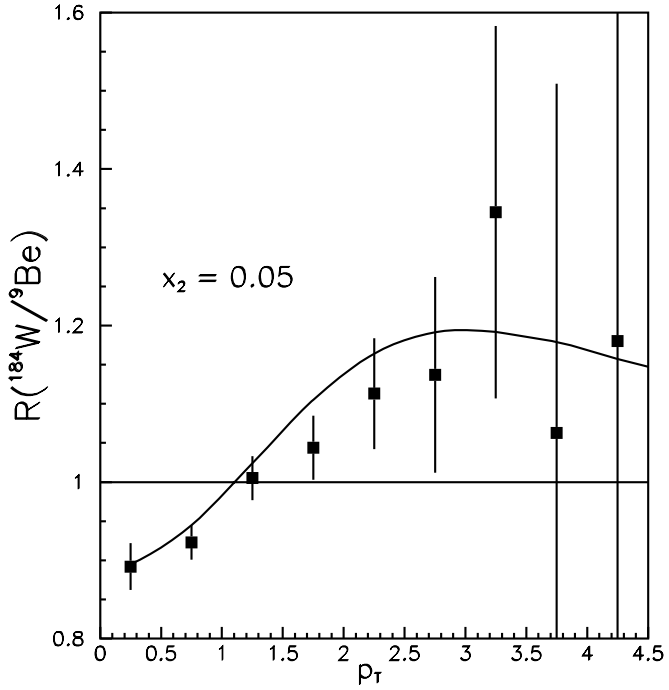

Fig. 3. Comparison of theoretical prediction of $R^{W/Be}(p_T)$ vs. p_T (in GeV/c) to experiment for $x_2 = 0.05$. Data are from the FermiLab E772/E866 collaboration [15,14,19]

The dependence of the quantity $\delta\langle p_T^2\rangle$ on A has been studied experimentally using the E772 data in [20]. They found that for large A,

$$\delta\langle p_T^2\rangle_{exp}^A \approx 0.021 A^{1/3} GeV^2. \tag{20}$$

We can make a calculation of the same quantity in the theory just described. From (16) we easily find that

$$\sigma_{DY}^A(p_T) = \frac{1}{\bar{\alpha}^2}\int d^2r_T e^{ip_T\cdot r} W^A(r_T)\sigma_{DY}^p(r_T) \tag{21}$$

where

$$W^A(r_T) = e^{-\frac{1}{2}\sigma_{\bar{q}q}(r_T)T_A(b,z)} \tag{22}$$

and

$$\sigma_{DY}^A(r_T) = \int d^2p_T e^{-p_T\cdot r_T}\sigma_{DY}^A(p_T) \tag{23}$$

characterizes how a quark acquires transverse momentum as it propagates through the nucleus. From (19, 21) we find

$$\langle p_T^2\rangle^A = -\frac{\nabla^2\sigma_{DY}^p(r_T)}{\sigma_{DY}^p(r_T)}|_{r_T=0} - \frac{\nabla^2 W^A(\bar{\alpha}r_T)}{W^A(\bar{\alpha}r_T)}|_{r_T=0} \tag{24}$$

The first term in (24), the mean-square momentum on a nucleon, is formally infinite. Fortunately, the nucleon contribution gets subtracted to obtain $\delta\langle p_T^2\rangle$,

$$\delta\langle p_T^2\rangle = -\bar{\alpha}^2\frac{\nabla^2 W^A(r_T)}{W^A(r_T)}|_{r_T=0}. \tag{25}$$

Note that the shadowing contribution in (12), which we justified in dropping by going to $x_2 > 0.05$, leads to a divergent contribution that no longer cancels exactly; in cases where FSI are important other means are needed to define a meaningful quantity [9].

Using (22), along with the observation that $\sigma_{\bar{q}q}(r_T)$ is proportional to r_T^2 at small r_T (see (5)),

$$\delta\langle p_T^2\rangle = \bar{\alpha}^2 C\langle T_A\rangle \tag{26}$$

where we have used the average of T_A as given in (18).

We may now make estimates to compare with the experimental result in (20). Using values of $C \approx 4-5$ as obtained from the GW or KST models, and taking the sharp-surface model for the nuclear density,

$$\langle T_A\rangle = \frac{3}{2}\rho_0 R_A \tag{27}$$

where $\rho_0 \approx 0.16 fm^{-3}$ is the central density of heavy nuclei and $R_A \approx 1.1A^{\frac{1}{3}}$, we find from theory that

$$\delta\langle p_T^2\rangle_{Th}^A \approx 0.047 A^{\frac{1}{3}}\ GeV^2 \tag{28}$$

The theoretical result in (28) is clearly larger than and in apparent disagreement with the experimental result in (20) [17,21]. However, it has been pointed out [22] that large systematic errors must be included in (20) and that when these are taken into account, the result in (28) could be accommodated.

3.4 Predictions for maximal shadowing

As we have stated, the case of maximal shadowing corresponds to $\ell_c \gg R_A$, and experiments in this regime have not yet been possible. The color dipole approach in the target rest frame applies in this limit, and numerous predictions have been presented in [9]. We give one example in Fig. 4, namely the DY ratios as a function of transverse momentum presented separately for longitudinal (L) and transverse + longitudinal ($T+L$) photon polarization.

In contrast to the weak shadowing limit discussed earlier, transverse momentum broadening here is associated with interactions with the quark following the emission of $\gamma*$. Note that the Cronin peak is much less visible in the LCL, which is a consequence of the gluon shadowing. For evaluating the gluon shadowing here, the Green's function method is required, and we take R_G from the calculations of [23].

4 Summary and conclusions

We have shown that the color dipole approach formulated in the target rest frame has advantages for examining nuclear modifications in $p+A$ collisions because the effects of shadowing may be determined theoretically. In the SCL, $\ell_c \ll R_A$, energy loss and momentum broadening are mediated by multiple interactions of the incident quark with target nucleons before the emission of the $\gamma*$. Analysis of the E772/E866 FermiLab experimental DY data at

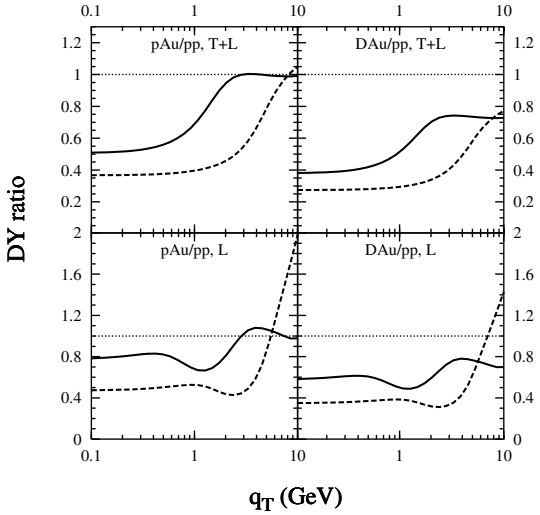

Fig. 4. Nuclear effects on the DY transverse momentum distribution. *Curves* show the DY cross sections for pAu (*left*) and deuterium – gold (*right*) collisions per nucleon divided by the DY cross section from pp scattering. *Solid curves* are predictions for RHIC ($\sqrt{s} = 200$ GeV) and *dashed* for LHC ($\sqrt{s} = 5.5$ TeV). Calculations are for M=4.5 GeV and $x_F = 0.5$

$E_p = 800\ GeV$ in the color dipole approach has provided improved determinations of these quantities, giving

$$\frac{dE_q}{dz} = -2.73 \pm 0.35\ GeV/fm \tag{29}$$

and

$$\delta\langle p_T^2\rangle \approx 0.047 A^{\frac{1}{3}}\ GeV^2 \tag{30}$$

The value of the rate of energy loss is larger than previous determinations, and the value of $\delta\langle p_T^2\rangle$ is about twice as large as the conventional value.

Predictions of the transverse momentum dependence of DY cross sections, for $p + A$ and $A + A$ collisions, have been made in the color dipole approach. These provide tests of the theory in a new physical regime of strong shadowing, where $\ell_c \gg R_A$, that may be explored at the LHC in the future.

Acknowledgements. I would like to acknowledge the essential contributions of my theoretical and experimental collaborators B. Kopeliovich, A. Tarasov, J. Raufeisen J. Moss, M. Leitch, and P. McGaughey. This work was supported in part by U.S. Department of Energy.

References

1. B.Z. Kopeliovich J. Raufeisen, and A.V. Tarasov: Phys. Lett. B **440**, 151 (1998); J. Raufeisen, A.V. Tarasov, and O.O. Voskresenskaya: Eur. Phys. J. A **5**, 173 (1999)
2. B.Z. Kopeliovich: Proc. of the Workshop Hirschegg '95: Dynamical Properties of Hadrons in Nuclear Matter, Hirschegg, January 16–21, 1995, ed. by H. Feldmeyer and W. Nörenberg, Darmstadt, 1995, p. 102 (hep-ph/9609385)
3. S.J. Brodsky, A. Hebecker, and E. Quack: Phys. Rev. D **55**, 2584 (1997)
4. K. Goltec-Biernat and M. Wüstoff: Phys. Rev. D **59**, 014017 (1999) (hep-ph/9807513); Phys. Rev. D **60**, 114023 (1999) (hep-ph/9903358)
5. B.Z. Kopeliovich, A. Schäfer, and A.V. Tarasov: Phys. Rev. C **59**, 1609 (1999) (hep-ph/9908245)
6. J. Raufeisen, J-C. Peng, and G. Nayak: Phys. Rev. D **66**, 034024 (2002) (hep-ph/0204095); B.Z. Kopeliovich, J. Raufeisen, and A.V. Tarasov: Phys. Lett. B **503**, 91 (2001); M.A. Betemps, M.B. Gay Ducati, M.V.T. Machado, and J. Raufeisen: Phys. Rev. D **67**, 114008 (2003)
7. J. Webb: New Mexico State University Thesis (2002) (hep-ex/0301031)
8. M.B. Johnson et al.: Phys. Rev. Lett. **86**, 4483 (2001) (hep-ex/0010051) and M.B. Johnson et al.: Phys. Rev. C **65**, 025203 (2002) (hep-ph/0105195)
9. B.Z. Kopeliovich, J. Raufeisen, A.V. Tarasov, and M.B. Johnson: Phys. Rev. C **67**, 025203 (2003) (hep-ph/0105195)
10. V.N. Gribov: Sov. Phys. JETP **29**, 483 (1969); **30**, 709 (1970)
11. V. Karmanov and L.A. Kondratyuk: Sov. Phys. JETP Lett. **18**, 266 (1973)
12. B.Z. Kopeliovich, J. Raufeisen, and A.V. Tarasov: Phys. Rev. C **62**, 035204 (2000)
13. D.M. Alde et al.: Phys. Rev. Lett. **66**, 133 (1991)
14. Unpublished E772 data
15. M.A. Vasiliev et al.: Phys. Rev. Lett. **83**, 2304 (1999)
16. Results shown in this subsection are preliminary. M.B. Johnson and B.Z. Kopeliovich: unpublished
17. M.B. Johnson, B.Z. Kopeliovich, and A.V. Tarasov: Phys. Rev. C **63**, 035203 (2001) (hep-ph/0006326)
18. Erratum to P. McGaughey et al.: Phys. Rev. D **50**, 3038 (1994)
19. M. Leitch: private communication
20. P.L. McGaughey, J.M. Moss, and J-C. Peng: Annu. rev. Nucl. Part. Sci. **49**, 217 (1999)
21. J. Raufeisen: Phys. Lett. B **557**, 184 (2003)
22. Joel Moss: private communication
23. B.Z. Kopeliovich, A. Schäfer, and A.V. Tarasov: Phys. Rev. D **62**, 054022 (2000) (hep-ph/9908245)